Original Research

Vadose Zone Journal

A Soil Water Repellency Empirical Model

Carlos M. Regalado* and Axel Ritter

The contact angle (α) varies nonlinearly with the soil water content (θ_g) in water-repellent soils; however, a quantitative description of such a θ_g dependence of α is still lacking. Using a dimensionality reduction technique such as dynamic factor analysis (DFA), we managed to identify two common patterns within a scattered data set of α vs. θ_g measurements performed with the molarity of an ethanol droplet test in 16 soil samples. These two common patterns, derived from the DFA, provided the basis for calibrating a proposed empirical, three-parameter, linear model that described satisfactorily (R^2 > 0.89) an additional α–θ_g data set used for model validation, from 40 soil samples with organic matter contents spanning from 110 to 650 g kg^{-1}. This offered both scaling and a flexible quantitative description of the soil water content dependence of water repellency.

Abbreviations: AIC, Akaike's information criterion; DFA, dynamic factor analysis; DFM, dynamic factor model; MED, molarity of an ethanol droplet; WR, water repellency.

As we advance in our understanding of soil water repellency (WR) dynamics, new questions arise as a consequence of more WR data becoming available. In this respect, results have accumulated in the past that indicate that soil WR depends on the gravimetric soil water content, θ_g, in a nonlinear fashion, i.e., soils are wettable close to field capacity and as θ_g diminishes, they become increasingly repellent up to a local or global WR maximum near the wilting point; from this peak onward, WR decreases monotonically or rises again near the oven-dry state (King, 1981; Wallis et al., 1990; de Jonge et al., 1999, 2007; Goebel et al., 2004; Regalado and Ritter, 2005; Kawamoto et al., 2007). Even though different degrees of WR have been often referred to as being more the rule than the exception in soils, there is not yet a model that fully describes such WR variation with soil moisture. There has been, however, a recent attempt to partially describe quantitatively such WR–θ_g behavior (Bachmann et al., 2007), but description has been generally merely qualitative, although some useful curve shape WR parameters have been proposed by Regalado and Ritter (2005). The idea of a WR model is appealing, if one takes into account that soil WR is involved in many important hydrologic processes, from land erosion to soil permeability, preferential flow, and soil water evaporation, and that therefore quantification and parameterization of the WR–θ_g phenomena would be very useful. For instance, once a WR model is available, we would be able to compare in quantitative terms WR–θ_g responses from different soils or make predictions of the WR status at unmeasured θ_g values within the soil moisture range from saturation to oven dryness. The reason why there exists no quantitative description of the variation of WR with θ_g in soils may possibly stem from the fact that the mechanisms leading to WR are not yet fully understood (Roberts and Carbon, 1971; Wallis et al., 1990; Doerr and Thomas, 2000; Doerr et al., 2002; Goebel et al., 2004). Additionally, if WR–θ_g measurements from different soil samples are plotted together, because of data dispersion, it is difficult to ascertain by visual inspection whether any WR patterns are shared by all samples (apart from the qualitative description already provided above) or whether a single curve may be able to describe the whole WR–θ_g data set. This is somehow connected to the classical problem of scaling in soil science and hydrology, whereby a scattered data set coalesces into a representative average reference curve derived for different soil types or spatial locations based on scaling considerations. Some illustrative examples are those of the scaled unsaturated hydraulic conductivity and water retention curves (Warrick et al., 1977; Russo and Bresler, 1980).

Instituto Canario de Investigaciones Agrarias (ICIA), Dep. Suelos y Riegos, Apdo. 60 La Laguna, 38200 Tenerife, Spain. Received 13 June 2008. *Corresponding author (cregalad@icia.es).

Vadose Zone J. 8:136–141
doi:10.2136/vzj2008.0097

Different tools have been developed for scaling soil-related properties, and these are of two basic types: empirical methods and dimensional analysis (Pachepsky et al., 2003). Some drawbacks of these methods are that in some instances scaling parameters are subjectively chosen by trial and error (Regalado, 2005); they presume a more or less relaxed physical (self-) similarity of the system (Miller and Miller, 1956; Pachepsky et al., 2000), or the functional form of the scaling laws must be known in advance or be derived ad hoc (Warrick, 1990). There exist other scaling techniques such as DFA (Zuur et al., 2003). Dynamic factor analysis is a dimensionality reduction statistical technique that can handle nonstationary, regularly spaced short series, with or without missing values, that has been classically applied to detect common trends in time-dependent series, originally from economics (Geweke, 1977) and more recently in hydrology (Muñoz-Carpena et al., 2005; Ritter and Muñoz-Carpena, 2006; Ritter et al., 2007), but whose potential as a dimensionality reduction tool for scaling time-independent problems has been overlooked. Advantages of the DFA are that it does not require a priori information about the underlying scaling laws, and that explanatory variables consisting of other observed series may be incorporated into the analysis as auxiliary variables to assist the description of the observed variability. In this study, we made use of DFA to show that this technique is useful as a scaling tool of a selected scattered WR–θ_g data set, providing clues about a flexible empirical model to describe WR in soils.

Materials and Methods

Soil Water Repellency Characterization

Fifty-six soil samples were selected from the top organic layer of a forested watershed in the Garajonay National Park, La Gomera (28°6′ N, 17°8′ W), Canary Islands, Spain, which was previously described in Regalado and Ritter (2005). Soil samples were first hand sieved (<2 mm) at field moisture and wetted until fully saturated in the lab. Then the molarity of an ethanol droplet (MED) test (Roy and McGill, 2002) was performed in desorption steps as described in Regalado and Ritter (2005), rendering 56 sets of α (°) vs. θ_g (kg kg^{-1}) data pairs. Following Regalado and Ritter (2005), we defined the following α–θ_g curve shape parameters: S (° kg kg^{-1}) is the trapezoidal integrated area enclosed between the α–θ_g curve and the α = 90° line; $\theta_{g\text{-max}}$ (kg kg^{-1}) is the soil water content at which α is maximum (α_{max}), and $\theta_{g\text{-min}}$ (kg kg^{-1}) is the wetted soil state at which WR is triggered; finally, the contact angle in the oven-dried soil is referred as $\alpha_{105°C}$ (°).

Dynamic Factor Analysis

Sets of α–θ_g data pairs were analyzed using DFA (Zuur et al., 2003). The DFA was performed with n = 16 out of the 56 sets of α vs. θ_g data pairs, with θ_g as the independent variable and α as the dependent one. Notice that the inverse problem would lead to a nonunique definition of the series. Since DFA can handle time series with missing values, gaps in the α–θ_g data were treated as unmeasured values, such that all the $\alpha(\theta_g)$ series were to have the same θ_g length. Dynamic factor analysis was originally designed for identifying underlying common patterns or latent unexplained effects in series of measured data of N response variables (in our case the 16 α–θ_g series), such that the following multiple linear model may be proposed (Lütkepohl, 1991; Zuur et al., 2003):

$$N \text{ response series} = \text{linear combination of M common patterns} + \text{level parameter} + \text{noise} \qquad [1]$$

When readily available, explanatory auxiliary variables may be also included in Eq. [1], although these were not considered in our case. Mathematically, Eq. [1] may be written in terms of the following dynamic factor model (DFM):

$$\boldsymbol{\alpha}_n\left(\theta_g\right)=\sum_{m=1}^{M}\gamma_{m,n}t_m\left(\theta_g\right)+\mu_n+\varepsilon_n\left(\theta_g\right) \qquad [2]$$

$$t_m\left(\theta_g^i\right)=t_m\left(\theta_g^{i-1}\right)+\eta_n\left(\theta_g^i\right) \qquad [3]$$

where $\boldsymbol{\alpha}_n(\theta_g)$ (n = 1, 2, …, N = 16) is the vector that contains the series of measured contact angle values at each ith soil water content θ_g; $t_m(\theta_g)$ is an M (<N) length vector gathering the common unknown patterns, such that DFA aims to explain most of the variability with the minimum possible M; the weighting factors $\gamma_{m,n}$ are referred to as factor loadings, and depending on their size one may identify what patterns are mainly responsible for each of the $\boldsymbol{\alpha}_n(\theta_g)$ response series; the constant-level parameters μ_n shift up and down each linear combination of common patterns; and $\varepsilon_n(\theta_g)$ and $\eta_m(\theta_g)$ are (independent) Gaussian noise distributions with zero mean and unknown (diagonal) covariance matrix. Parameters in the DFM Eq. [2–3] were optimized with the expectation maximization (EM) algorithm (Dempster et al., 1977; Shumway and Stoffer, 1982; Wu et al., 1996). The $t_m(\theta_g)$ patterns were modeled as a random walk (Harvey, 1989) and were estimated using the Kalman filter–smoothing algorithm and the EM algorithm (Zuur and Pierce, 2004). Since DFA is readily implemented in the Brodgar version 2.5.6 package (Highland Statistics Ltd., Newburgh, UK; www.brodgar.com, verified 21 Nov. 2008), that software was used in this study. A more detailed description of DFA techniques may be found in Zuur et al. (2007).

The best DFM was selected in terms of the coefficient of efficiency, C_{eff} (Nash and Sutcliffe, 1970), and Akaike's information criterion (AIC), an index that penalizes overparameterization in a better fitting model, such that usually the preferred model is that with the smallest AIC (Akaike, 1974). Additionally, cross-correlation between $\boldsymbol{\alpha}_n(\theta_g)$ and $t_m(\theta_g)$ was quantified by means of the so-called canonical correlation coefficients, $\rho_{m,n}$, such that a $\rho_{m,n}$ close to unity implies that a specified mth common pattern is strongly associated with a particular $\boldsymbol{\alpha}_n(\theta_g)$ (n = 1, 2, …, 16). Furthermore, when $|\rho_{m,n}| < 0.30$, $\boldsymbol{\alpha}_n(\theta_g)$ and $t_m(\theta_g)$ correlation may be considered negligible, while when $0.30 \le |\rho_{m,n}| < 0.50$ correlation is considered to be low, moderate if $0.50 \le |\rho_{m,n}| \le 0.75$, and high if $|\rho_{m,n}| > 0.75$.

Results and Discussion

Exploratory Analysis of the Water Repellency Curves

Figure 1 depicts the 16 α–θ_g data sets obtained with the MED test and used in the DFA. Some samples almost recovered their wettability under oven-dried conditions, i.e., $\alpha_{105°C} \sim 90°$, while others remained repellent when dried; WR was triggered in

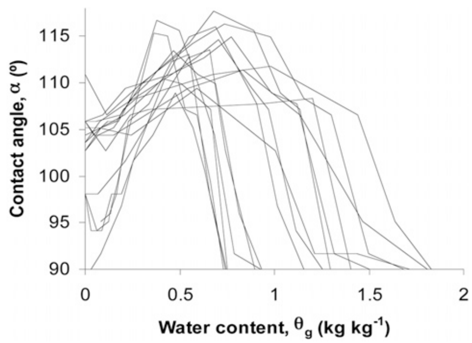

FIG. 1. Variation of contact angle with the soil water content for the 16 soil samples used in the dynamic factor analysis and model calibration.

TABLE 1. Selection of dynamic factor models based on performance coefficients (Akaike's information criterion, AIC, and the coefficient of efficiency, C_{eff}).

No. of patterns (M)	AIC†	C_{eff}
1	1298	0.772
2	1205	0.929
3	1121	0.972
4	1122	0.976

† The lowest number represents the best model.

a wide range of soil water contents, such that some soil samples initiated their repellency earlier than others. This all translates into the large data dispersion observed in Fig. 1, and consequently this is reflected in the WR curve shape parameters, such that S ranged from 7 to 30° kg kg^{-1}, $\theta_{g\text{-max}}$ varied from 0.36 to 1.20 kg kg^{-1} and α_{max} spanned 108 to 118°, the minimum $\theta_{g\text{-min}}$ observed was 0.73 kg kg^{-1} while maximum $\theta_{g\text{-min}}$ was 1.83 kg kg^{-1}, and $\alpha_{105°C}$ extended from 90 to 111°.

Scaling and Dynamic Factor Analysis

The dimensionality reduction of the α–θ_g data shown in Fig. 1 was performed with DFA by identifying common patterns in sequential steps. Table 1 summarizes the AIC and C_{eff} values obtained as the number of common patterns was incremented, such that the best DFM, i.e., the lowest AIC, was the one with $M = 3$, although a slight improvement was obtained in terms of the C_{eff} for $M = 4$. No further model enhancement was achieved beyond $M = 4$. Although the preferred DFM is the one with $M = 3$, the $M = 2$ model has the advantage of being simpler and the goodness of fit is still acceptable and this will be explored below. Figures 2 and 3 show the common patterns and canonical correlation coefficients for $M = 2$ and $M = 3$, respectively. Figure 2a and 2c depict two similar patterns but mirror images and slightly displaced with respect to the θ_g axis. This is also the case for $M = 3$, but a third pattern appears more random at intermediate θ_g values where most of the structure of the other two trends appears (Fig. 3a, 3c, and 3e); it is in this intermediate moisture region where soil WR is more relevant (Fig. 1). With respect to the canonical correlation coefficients, in general both trends are associated with WR for almost all samples when $M = 2$, i.e., $|\rho_{m,n}| > 0.3$; the first pattern may be strongly associated with Samples 3 and 6 through 16; by contrast, the second pattern is highly correlated, i.e. $|\rho_{1,n}|$>0.75, with Samples 1 through 5, 14, and 16 (Fig. 2b and 2d). In the case of $M = 3$, $\rho_{1,n}$ and $|\rho_{2,n}|$ are also >0.3 for all samples, exhibiting moderate to high correlation with the first two in most cases (Fig. 3b and 3d); however, the third pattern appears less relevant for some samples, with $|\rho_{3,n}|$ being >0.3 for Samples 6 through 13 and 15; the canonical correlation coefficient $\rho_{3,2} = 0$, thus this last pattern is not necessary to explain the WR behavior of Sample 2 (Fig. 3f). It is also noticeable that $|\rho_{1,n}|$ and $\rho_{3,n}$ were linearly correlated with the area enclosed between the α–θ_g curve and the line $\alpha = 90°$ ($R^2 > 0.85$), such that as S increased, the first and third patterns became less relevant. Thus we may conclude that soil WR of a wide variety of α–θ_g curve shapes may be described with two common underlying latent effects only, and that a third pattern may be necessary for the soil water regime close to saturation where WR may be less apparent.

A Soil Water Repellency Empirical Model

Based on the above DFA, we derived an empirical model of soil WR to describe the θ_g dependence of α. This was done in two steps. First, Patterns 1 (P_1) and 2 (P_2) derived from the DFA (Fig. 2a and 2c) were modeled by nonlinear fitting, to provide a mathematical description of the discrete P_1 and P_2 series rendered by the Brodgar software. The objective of this study was to develop a

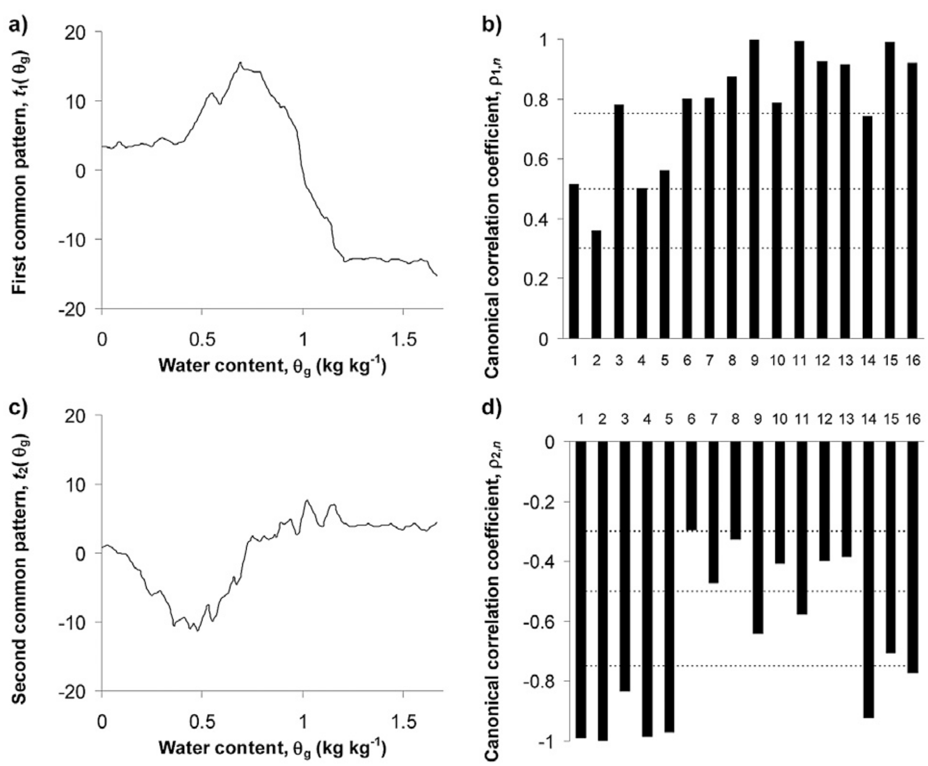

FIG. 2. (a, c) Common patterns and (b, d) canonical correlation coefficients ($\rho_{m,n}$) for the dynamic factor model with the number of common patterns $M = 2$.

model that describes the α–θ_g curve. Thereby it is useful to have an analytical description of the DFA patterns in terms of θ_g. This explains why, in the following, we used a smoothed version of the DFA patterns and not the DFA patterns themselves, such that

$$P_m = \frac{a + c\theta_g + e\theta_g^2 + g\theta_g^3 + i\theta_g^4 + k\theta_g^5}{1 + b\theta_g + d\theta_g^2 + f\theta_g^3 + h\theta_g^4 + j\theta_g^5} \quad [4]$$

was found to fit satisfactorily ($R^2 \geq 0.97$) both common patterns (Table 2). Given the nonlinear behavior of WR vs. soil water content, the fitting of a highly parameterized rational polynomial to both patterns is somehow justified. The main issue here, however, is that DFA permits the identification of common patterns that are not quantifiable by visual inspection, and that fitting of these patterns is done only once during model calibration (with an N = 16 subsample). Next, and according to the DFM Eq. [2], a multiple linear model was developed and fitting parameters optimized for 40 additional α–θ_g data sets used as validation of the model.

TABLE 2. Fitting parameters and goodness-of-fit criteria of the model Eq. [4] for the two common patterns shown in Fig. 2a and 2c.

Parameter	Pattern 1	Pattern 2
a	3.30	1.16
b	−5.74	−7.25
c	−16.88	−18.02
d	12.57	20.73
e	30.75	66.45
f	−12.42	−18.79
g	−23.48	−133.66
h	5.11	−9.26
i	13.06	85.15
j	−0.45	18.22
k	−6.69	20.89
R^2	0.99	0.97

Model Eq. [2] (without the noise term) was thus selected as the basis for a general empirical WR model such that

$$\alpha_n(\theta_g) = \nu_{1,n} P_1(\theta_g) + \nu_{2,n} P_2(\theta_g) + \nu_{3,n} \quad [5]$$

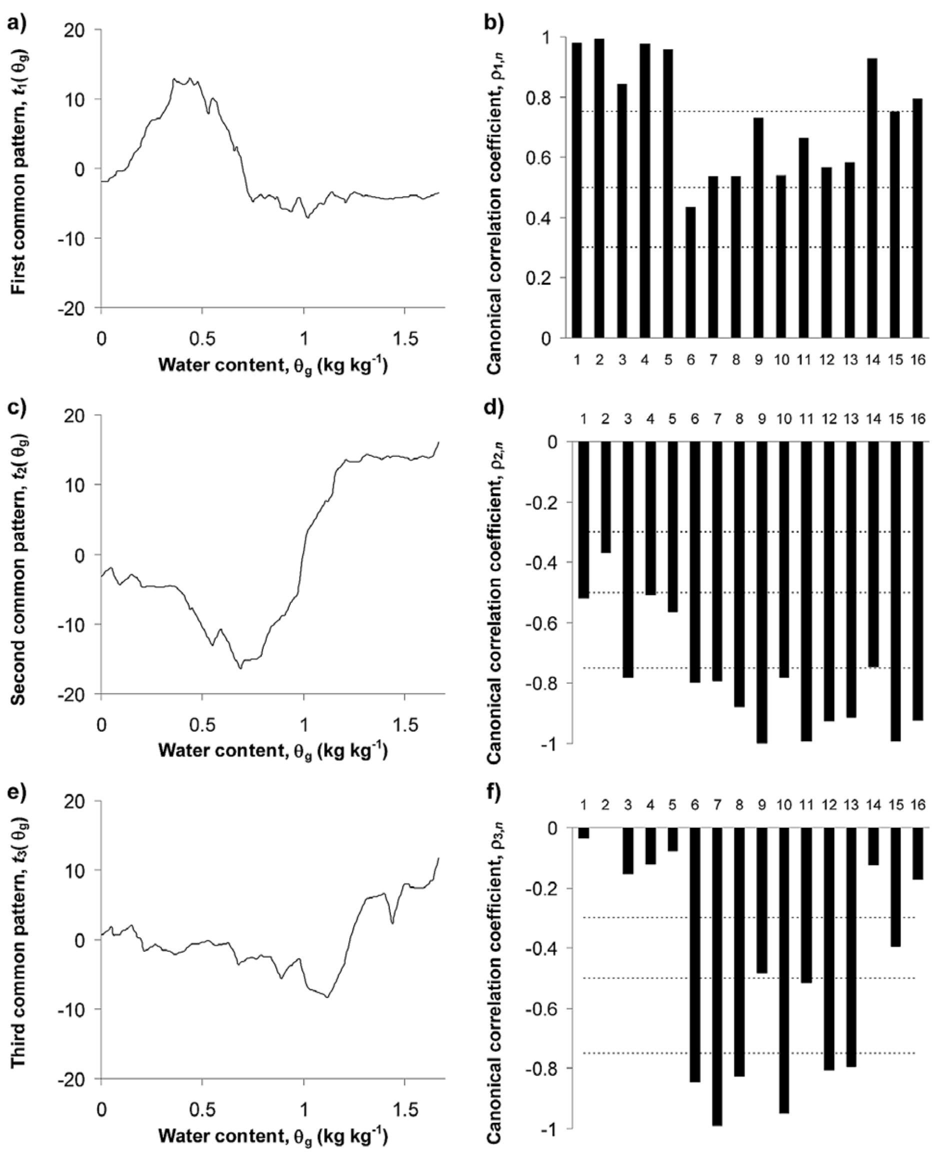

FIG. 3. (a, c, e) Common patterns and (b, d, f) canonical correlation coefficients ($\rho_{m,n}$) for the dynamic factor model with the number of common patterns M = 3.

where $\nu_{i,n}$ are n-length vectors of fitting parameters. Thus, model validation (Eq. [5]) only requires fitting of three parameters (ν_1, ν_2, and ν_3) for each soil sample and the parameters in Eq. [4] are only fitted once during the calibration of the model. Figure 4 illustrates the outcome of the fitted model for the 40 soil samples selected for model validation, showing the good correspondence between measured and predicted WR values ($R^2 > 0.89$). Since the MED test is only sensitive for contact angles >90° only α > 90° points are shown in Fig. 4. The large variety of curve shapes successfully fitted by the model shows its flexibility and generality given the wide range of soil organic matter content exhibited by the 40 soil samples, i.e., 110 to 650 g kg^{-1}. We may stress that the satisfactory fitting outcome shown in Fig. 4 is achieved with only three fitting parameters (ν_1, ν_2, and ν_3) for each sample. Another issue is related to possible relations between model parameters and soil properties. The proposed model is empirical, however, and any connection between fitting parameters and soil properties may be simply coincidental. The only soil property determined for all soil samples was the organic matter content, and no unequivocal relationship was observed between the soil organic matter content and the ν_i parameters (results not shown).

Conclusions

Lacking a mechanistic understanding of soil WR, we have approached modeling the water content dependence of the

Fig. 4. Empirical models Eq. [4–5] fitted to the 40 measured contact angle α–water content θ_g data sets used for model validation.

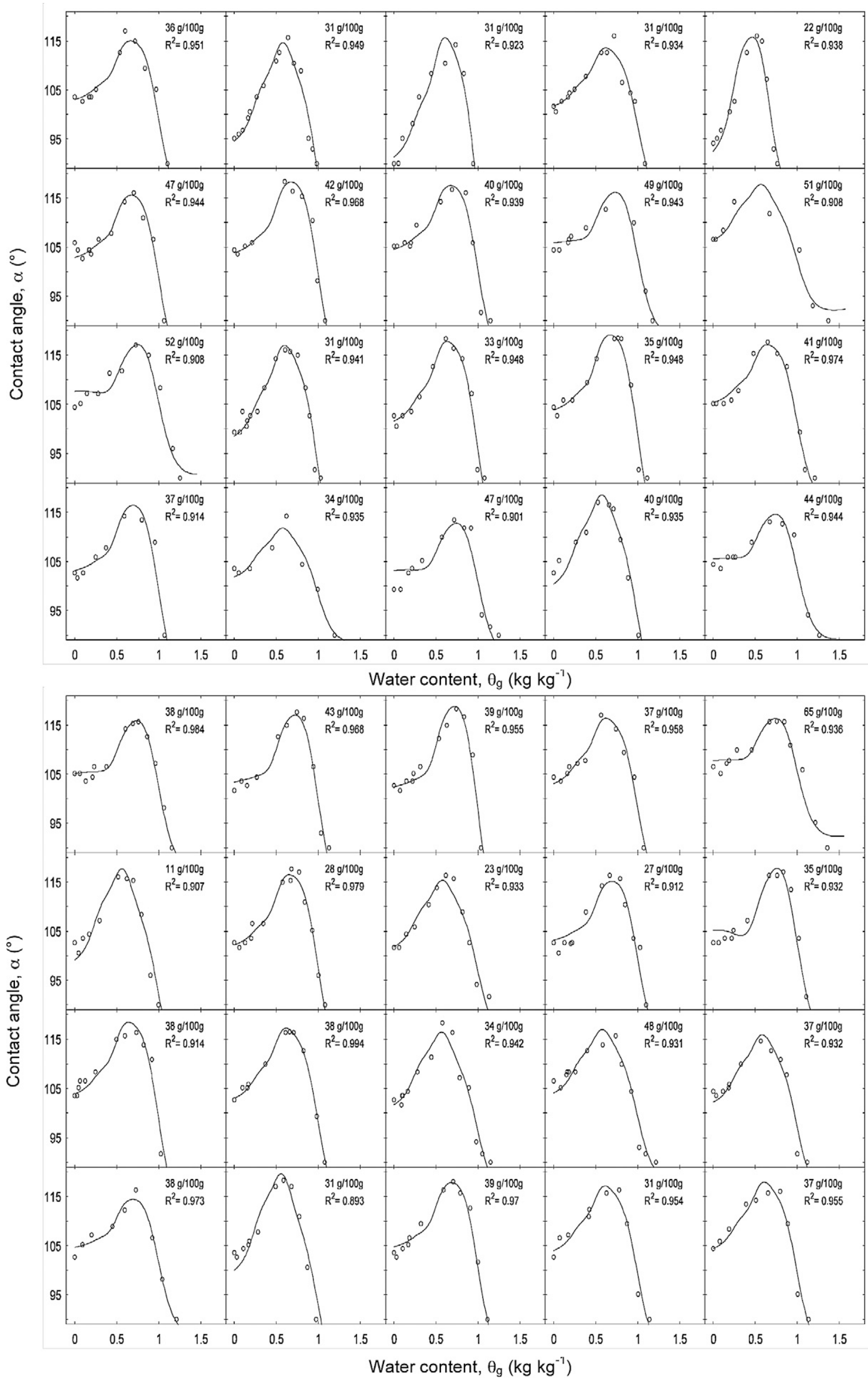

contact angle by means of DFA, which permitted us to identify two common patterns representing unexplained variability. Using those two patterns recognized by DFA as the seed for a general WR-characterizing model, a multiple linear empirical model was derived that successfully described the α–θ_g dependence of 40 soil samples with organic matter contents from 110 to 650 g kg^{-1}. These are considered a representative family of α–θ_g forms given the wide range of soil organic matter and curve shapes exhibited, and therefore the flexibility and generality of the proposed model is ensured. This provides the basis for further application of the derived model in other soils with different textures to prove its universality. Furthermore, the nonlinearity of WR–θ_g measurements is not exclusive to the MED test but is also representative of the water drop penetration time (WDPT) test, which characterizes the WR of the soil in terms of persistence instead of contact angle, and therefore the proposed techniques used here may well be applied in deriving an equivalent WDPT–θ_g model.

Acknowledgments

This work was financed by the INIA-Programa Nacional de Recursos y Tecnologías Agroalimentarias (Project RTA2005-228). A. Ritter would like to acknowledge financial support from the European Social Fund.

References

Akaike, H. 1974. A new look at the statistical model identification. IEEE Trans. Automat. Control 19:716–723.

Bachmann, J., M. Deurer, and G. Arye. 2007. Modeling water movement in heterogeneous water-repellent soil: 1. Development of a contact angle-dependent water-retention model. Vadose Zone J. 6:436–445.

de Jonge, L.W., O.H. Jacobsen, and P. Moldrup. 1999. Soil water repellency: Effects of water content, temperature, and particle size. Soil Sci. Soc. Am. J. 63:437–442.

de Jonge, L.W., P. Moldrup, and O.H. Jacobsen. 2007. Soil-water content dependency of water repellency in soils: Effect of crop type, soil management, and physical-chemical parameters. Soil Sci. 172:577–588.

Dempster, A.P., N.M. Laird, and D.B. Rubin. 1977. Maximum likelihood from incomplete data via the EM algorithm. J. R. Stat. Soc. Ser. B 39:1–38.

Doerr, S.H., L.W. Dekker, C.J. Ritsema, R.A. Shakesby, and R. Bryant. 2002. Water repellency of soils: The influence of ambient relative humidity. Soil Sci. Soc. Am. J. 66:401–405.

Doerr, S.H., and A.D. Thomas. 2000. The role of soil moisture in controlling water repellency: New evidence from forest soils in Portugal. J. Hydrol. 231–232:134–147.

Geweke, J.F. 1977. The dynamic factor analysis of economic time series models. p. 365–382. *In* D.J. Aigner and A.S. Goldberger (ed.) Latent variables in socio-economic models. North-Holland, Amsterdam.

Goebel, M.-O., J. Bachmann, S.K. Woche, W.R. Fischer, and R. Horton. 2004. Water potential and aggregate size effects on contact angle and surface energy. Soil Sci. Soc. Am. J. 68:383–393.

Harvey, A.C. 1989. Forecasting, structural time series models and the Kalman filter. Cambridge Univ. Press, New York.

Kawamoto, K., P. Moldrup, T. Komatsu, L.W. de Jonge, and M. Oda. 2007. Water repellency of aggregate-size fractions of a volcanic ash soil. Soil Sci. Soc. Am. J. 71:1658–1666.

King, P.M. 1981. Comparison of methods for measuring severity of water repellence of sandy soils and assessment of some factors that affect its measurement. Aust. J. Soil Res. 19:275–285.

Lütkepohl, H. 1991. Introduction to multiple time series analysis. Springer-Verlag, Berlin.

Miller, E.E., and R.D. Miller. 1956. Physical theory of capillary flow phenomena. J. Appl. Phys. 27:324–332.

Muñoz-Carpena, R., A. Ritter, and Y.C. Li. 2005. Dynamic factor analysis of groundwater quality trends in an agricultural area adjacent to Everglades National Park. J. Contam. Hydrol. 80:49–70.

Nash, J.E., and J.V. Sutcliffe. 1970. River flow forecasting through conceptual models. Part 1. A discussion of principles. J. Hydrol. 10:282–290.

Pachepsky, Ya., J.W. Crawford, and W.J. Rawls (ed.). 2000. Fractals in soil science. Dev. Soil Sci. 27. Elsevier Science, Amsterdam.

Pachepsky, Ya., D.E. Radcliffe, and H.M. Selim (ed.). 2003. Scaling methods in soil physics. CRC Press, Boca Raton, FL.

Regalado, C.M. 2005. On the distribution of scaling hydraulic parameters in a spatially anisotropic banana field. J. Hydrol. 307:112–125.

Regalado, C.M., and A. Ritter. 2005. Characterizing water dependent soil repellency with minimal parameter requirement. Soil Sci. Soc. Am. J. 69:1955–1966.

Ritter, A., and R. Muñoz-Carpena. 2006. Dynamic factor modeling of ground and surface water levels in an agricultural area adjacent to Everglades National Park. J. Hydrol. 317:340–354.

Ritter, A., R. Muñoz-Carpena, D.D. Bosch, B. Schaffer, and T.L. Potter. 2007. Agricultural land use and hydrology affect variability of shallow groundwater nitrate concentration in South Florida. Hydrol. Processes 21:2464–2473.

Roberts, F.J., and B.A. Carbon. 1971. Water repellence in sandy soils of south-western Australia: II. Some chemical characteristics of the hydrophobic skins. Aust. J. Soil Res. 10:35–42.

Roy, J.L., and W.B. McGill. 2002. Assessing soil water repellency using the molarity of ethanol droplet (MED) test. Soil Sci. 167:83–97.

Russo, D., and E. Bresler. 1980. Scaling soil hydraulic properties of a heterogeneous field. Soil Sci. Soc. Am. J. 44:681–684.

Shumway, R.H., and D.S. Stoffer. 1982. An approach to time series smoothing and forecasting using the EM algorithm. J. Time Ser. Anal. 3:253–264.

Wallis, M.G., D.J. Horne, and K.W. McAuliffe. 1990. A study of water repellency and its amelioration in a yellow brown sand: 1. Severity of water repellency and the effects of wetting and abrasion. N.Z. J. Agric. Res. 3:139–144.

Warrick, A.W. 1990. Application of scaling to the characterization of spatial variability in soils. p. 39–51. *In* D. Hillel and D.E. Elrick (ed.) Scaling in soil physics: Principles and applications. SSSA Spec. Publ. 25. SSSA, Madison, WI.

Warrick, A.W., G.J. Mullen, and D.R. Nielsen. 1977. Scaling field-measured soil hydraulic properties using a similar media concept. Water Resour. Res. 13:355–362.

Wu, L.S.-Y., J.S. Pai, and J.R.M. Hosking. 1996. An algorithm for estimating parameters of state-space models. Stat. Prob. Lett. 28:99–106.

Zuur, A.F., R.J. Fryer, I.T. Jolliffe, R. Dekker, and J.J. Beukema. 2003. Estimating common trends in multivariate time series using dynamic factor analysis. Environmetrics 14:665–685.

Zuur, A.F., E.N. Ieno, and G.M. Smith. 2007. Analysing ecological data. Springer-Verlag, Berlin.

Zuur, A.F., and G.J. Pierce. 2004. Common trends in Northeast Atlantic squid time series. J. Sea Res. 52:57–72.